Original Article

Quantitative assessment of zonal trabecular volumetric bone mineral density in middle-aged and elderly women using quantitative computed tomography

Xingyuan Yang[1], Ying Liu[1#], Jing Liu[1], Lei Gao[1], Ping Zhang[1], Yan Wang[2#], Wei Zhang[1]

[1]Department of Radiology, The Third Hospital of Hebei Medical University, Shijiazhuang, China; [2]Department of Endocrinology, The Third Hospital of Hebei Medical University, Shijiazhuang, China

Contributions: (I) Conception and design: Y Liu, P Zhang, W Zhang; (II) Provision of study materials or patients: Y Wang; (III) Collection and assembly of data: X Yang, J Liu; (IV) Data analysis and interpretation: Y Liu, Y Wang, L Gao; (V) Manuscript writing: All authors; (VI) Manuscript minor and major revision: X Yang, Y Liu, Y Wang; (VII) Final approval of manuscript: All authors.

[#]These authors contributed equally to this work.

Correspondence to: Ying Liu. Department of Radiology, The Third Hospital of Hebei Medical University, 139 Ziqiang Street, Qiaoxi District, Shijiazhuang 050050, China. Email: 18503117687@163.com; Yan Wang. Department of Endocrinology, The Third Hospital of Hebei Medical University, 139 Ziqiang Street, Qiaoxi District, Shijiazhuang 050050, China. Email: wangyan66200@163.com.

Background: To explore the feasibility of the 9 zonal trabecular volumetric bone mineral density (trabecular vBMD) method in the first lumbar vertebral body (L1) and to assess the zonal trabecular vBMD distribution of L1 in women aged 50–80 years.

Methods: A total of 578 women patients underwent a quantitative computed tomography (CT) scan of the L1 vertebra, and these patients were categorized into 3 age subgroups with 10-year intervals. L1 was segmented into 9 zones, based on which, L1 was then divided into 6 regions [i.e., vBMD-anterior (vBMD-A), vBMD-medial (vBMD-M), and vBMD-posterior (vBMD-P) from the ventral to the dorsal side, vBMD-upper (vBMD-U), vBMD-medial (vBMD-M'), and vBMD-lower (vBMD-L) from the head to the foot]. Independent samples t-test, intraclass correlation coefficient (ICC), and one-way analysis of variance (ANOVA) were used for statistical analyses.

Results: There were no significant differences of the 9 zonal vBMDs measured by the 2 analysts ($P \geq 0.638$), and ICCs were all greater than or equal to 0.990. There was significant difference of global vBMD among the 3 age groups ($P<0.001$), and so as to the 9 zonal vBMDs among the 3 age groups ($P<0.001$). Age was negatively correlated with global vBMD and the 9 zonal vBMDs ($P<0.001$). There were significant differences among vBMD-A, vBMD-M, and vBMD-P ($P<0.001$), and vBMD-A and vBMD-M were both lower than vBMD-P. There were significant differences among vBMD-U, vBMD-M', and vBMD-L ($P<0.001$), and vBMD-U and vBMD-L were both lower than vBMD-M'.

Conclusions: The 9 zonal trabecular vBMD method of L1 is stable and feasible, and the 9 zonal trabecular vBMD method may quantitatively explain osteoporotic vertebral deformity from the perspective of vBMD in middle-aged and elderly women.

Keywords: Volumetric bone mineral density (v-BMD); quantitative computed tomography (QCT); osteoporotic vertebral deformity (OVF)

Submitted Jun 25, 2022. Accepted for publication Jan 19, 2023. Published online Mar 10, 2023.
doi: 10.21037/qims-22-575
View this article at: https://dx.doi.org/10.21037/qims-22-575

Introduction

Osteoporosis is characterized by low bone mass, microarchitectural deterioration, and fragility fractures and is a major clinical problem prevalent in elderly (≥65 years old) women and men (1). Impairments in physical functional, quality of life, and survival of vertebral body compression fracture secondary to osteoporosis are associated with the degree of spinal deformity (2). Spine radiographs, Genant's semiquantitative (GSQ) criteria, and the standardized semi-quantitative grading scale recommended by the International Osteoporosis Foundation and the International Society for Clinical Densitometry have been commonly used to identify vertebral deformity (VD) secondary to osteoporotic vertebral fracture (OVF) for vertebrae T4 to L4 for nearly 30 years. Each of the vertebrae from T4 to L4 is classified into 1 of the 4 grades according to Genant's score from Grade 0 to Grade 3. Grade 0 (normal), Grade 1 (mildly deformed, a 20–25% reduction in 1 of the 3 heights and a 10–20% reduction of area), Grade 2 (moderately deformed, a 25–40% reduction in any height and a reduction in area of 20–40%), and Grade 3 (severely deformed, a 40% or more reduction in height and area) (3).

Although dual X-ray absorptiometry (DXA) remains the diagnostic tool for osteoporosis preferred by the International Society for Clinical Densitometry (ISCD), DXA cannot be used in patients with scoliosis or abdominal aortic wall calcification caused by chronic diseases, and degenerative changes and osteophytes artificially elevate DXA results. Some patients who are not suitable for DXA examination may undergo a CT scan with or without other clinical purposes. At present, clinical quantitative computed tomography (QCT) with or without phantom calibration can assess bone quality without increasing radiant quantity and economic burden (4). QCT can measure 3-dimensional (3D) trabecular volumetric bone mineral density (trabecular vBMD, mg/cm^3) without being influenced by vertebral osteophytes, facet degeneration, disc stenosis, endplate sclerosis, and calcification of abdominal aortic wall (5).

The purpose of our study was to explore the feasibility of the 9 zonal trabecular vBMD method in the first lumbar vertebral body (L1) and to assess the zonal trabecular vBMD distribution of L1 in women aged 50–80 years.

Methods

Patient sample

We retrospectively reviewed a single-center database of QCT examinations between January 2017 and December 2019 with approval from the Ethics Committee of The Third Hospital of Hebei Medical University (No. ke2018-036-1). All participants provided written informed consent before QCT examination. The study was conducted in accordance with the Declaration of Helsinki (as revised in 2013). Women aged between 50 and 80 years were eligible to apply. The exclusion criteria included smoking and drinking alcohol, paralysis, history of malignant tumor, history of ovarian and/or uterine surgery, vertebral fracture and/or surgery of L1, and having a disease that influences bone metabolism, including renal failure, hyperthyroidism, and hyperparathyroidism and/or taking drugs affecting bone metabolism such as sex steroids, warfarin, and bisphosphonates. Finally, we included 578 female patients (64.0±8.47 years, between 50 and 80 years), and 58 patients were excluded (*Figure 1*). Participants were categorized into 3 age groups with 10-year intervals (50–59, 60–69, and 70–80 years). We recorded age, height, and weight, and height and weight were assessed using standard methods. Body mass index (BMI) was calculated as weight (kg) divided by height squared (m^2).

Image acquisition

All participants underwent a cross-sectional CT scan of L1 (from the 12th thoracic to the 2nd lumbar vertebra) in a supine position using a CT scanner (Somatom Sensation 64; Siemens, Erlangen, Germany) with hands above the head and a simultaneous solid Mindways QCT phantom (Mindways Software Inc., Austin, TX, USA) close to their dorsal side. CT scans was performed using the following parameters: kV =120, mAs =125, table height =168 cm, matrix = 512×512, slice thickness =1 mm, and field of view (FOV) =500 mm.

Image analysis

Images were transferred to the QCT workstation and analyzed using the Mindways software to measure volumetric bone mineral density (vBMD, mg/cm^3).

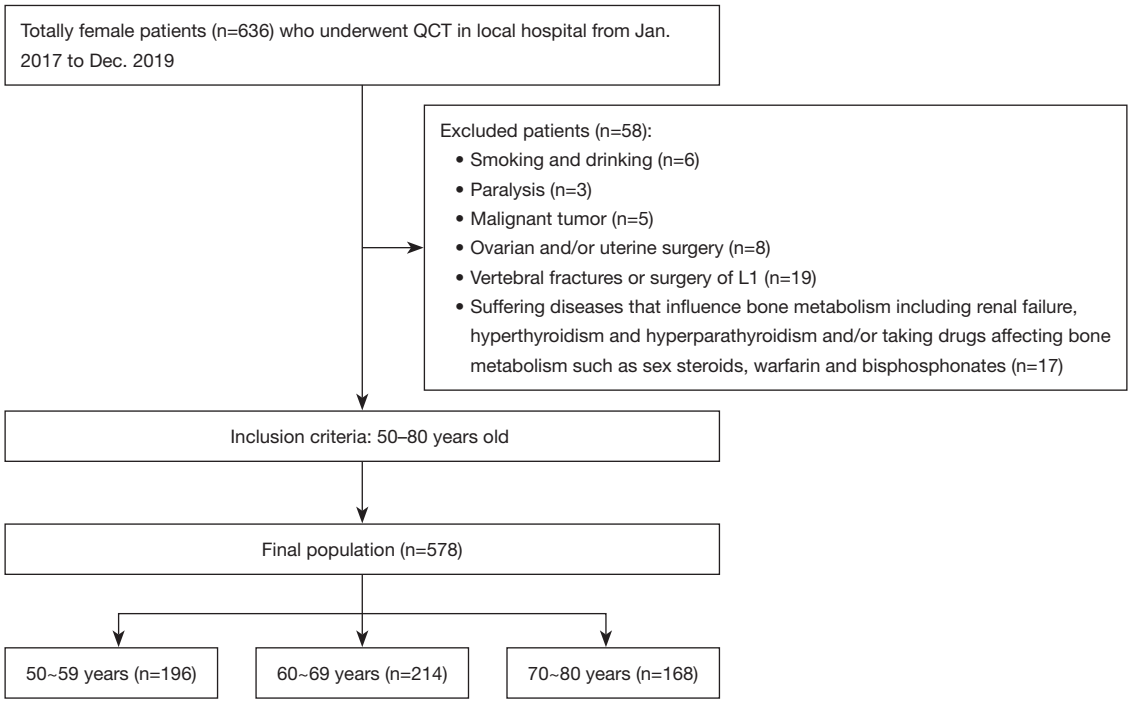

Figure 1 Flow chart illustrating the patient inclusion and selection process for this study. QCT, quantitative computed tomography.

Global vBMD

Global vBMD was defined as the whole vertebral body, with an elliptical region of interest (ROI) of about 250 mm^2 area and 9 mm height placed at the midplane of L1 avoiding the cortical bone and hyperostosis osteosclerosis (*Figure 2A*).

Nine zonal vBMDs

L1 was segmented into 9 zones, the upper and anterior (ua), upper and middle (um), upper and posterior (up), middle and anterior (ma), middle and middle (mm), middle and posterior (mp), lower and anterior (la), lower and middle (lm), and lower and posterior (lp), with each encompassing one third of the L1 vertebral body (*Figure 2B*,*2C*). An elliptical ROI with about 80 mm^2 area and 3 mm height was placed at each zone avoiding the cortical bone and hyperostosis osteosclerosis. The vBMD measurements of the 9 zones were defined as vBMD-ua, vBMD-um, vBMD-up, vBMD-ma, vBMD-mm, vBMD-mp, vBMD-la, vBMD-lm, and vBMD-lp (*Figure 2D-2L*).

Six regional vBMD

Based on 9 zonal vBMDs, we divided the L1 vertebral body into 6 regions: vBMD-A, vBMD-M, vBMD-P, vBMD-U, vBMD-M', and vBMD-L.

$$\begin{aligned}
&\text{vBMD-A} = (\text{vBMD-ua} + \text{vBMD-ma} + \text{vBMD-la})/3\\
&\text{vBMD-M} = (\text{vBMD-um} + \text{vBMD-mm} + \text{vBMD-lm})/3\\
&\text{vBMD-P} = (\text{vBMD-up} + \text{vBMD-mp} + \text{vBMD-lp})/3\\
&\text{vBMD-U} = (\text{vBMD-ua} + \text{vBMD-um} + \text{vBMD-up})/3\\
&\text{vBMD-M'} = (\text{vBMD-ma} + \text{vBMD-mm} + \text{vBMD-mp})/3\\
&\text{vBMD-L} = (\text{vBMD-la} + \text{vBMD-lm} + \text{vBMD-lp})/3
\end{aligned} \quad [1]$$

vBMD-A, vBMD-M, and vBMD-P were defined as vBMD of the anterior, middle, and posterior third of the L1 vertebral body from the ventral to the dorsal side. vBMD-U, vBMD-M', and vBMD-L were defined as vBMD of the upper, middle, and lower third of the L1 vertebral body from the head to the foot.

The feasibility of global and 9 zonal vBMDs, involving 30 volunteers (aged between 51 and 79 years old, 64.9± 8.8 years old), was assessed by 2 analysts (Xingyuan Yang, who was a resident with more than 3 years of QCT operation experience and Jing Liu, who was a technician with more than 3 years of QCT operation experience). After the feasibility of the global and 9 zonal vBMDs was established, only the global and 9 zonal vBMD values from the primary analyst were used.

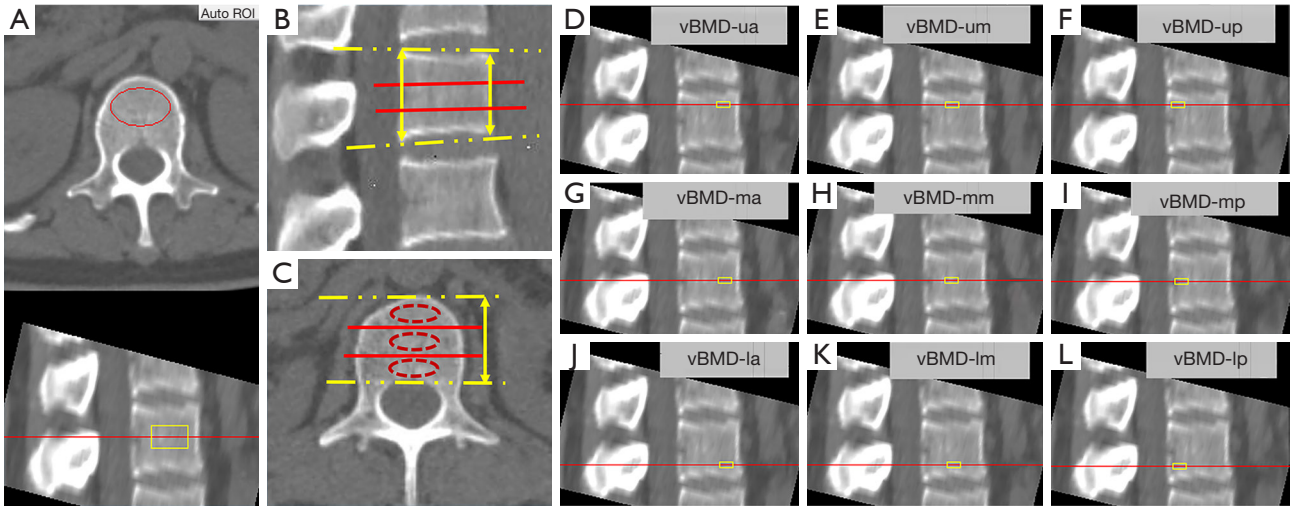

Figure 2 Regions of interest setting method of global vBMD and nine zonal segmentation method of L1. (A) Global vBMD measurement. An elliptical ROI of about 250 mm^2 area and 9 mm height placed at the midplane of L1. (B) Four boundary points of L1 are established at the maximum level of the sagittal vertebral body, then the anterior and posterior edge of L1 is established, and the anterior and posterior edge are divided into three equal parts. The upper third points of the anterior and posterior edges are connected, followed by the lower third points. Thus, L1 is divided into upper, middle, and lower zones from the head to the foot. (C) The anterior edge of L1 is established based on the tangent line of the vertebral anterior arc, followed by the posterior edge through the trailing edge and parallel to the anterior edge on the maximum level of the axial vertebral body. Then, the distance between the anterior and posterior edge is divided into three equal parts. Thus, L1 is divided into anterior, middle, and posterior zones from the ventral to the dorsal side. (D-L) Based on the sagittal and axial image segmentation method, L1 is divided into nine zones, the upper and anterior (ua), upper and middle (um), upper and posterior (up), middle and anterior (ma), middle and middle (mm), middle and posterior (mp), lower and anterior (la), lower and middle (lm), and lower and posterior (lp) third of L1. The vBMD of the nine zones were defined as vBMD-ua (D), vBMD-um (E), vBMD-up (F), vBMD-ma (G), vBMD-mm (H), vBMD-mp (I), vBMD-la (J), vBMD-lm (K), and vBMD-lp (L). An elliptical ROI of about 80 mm^2 area and 3 mm height was placed at each zone. ROI, region of interest; vBMD, volumetric bone mineral density; L1, first lumbar vertebral body.

Statistical analysis

SPSS 26.0 (IBM Corp., Armonk, NY, USA) statistical software package was used for statistical analysis. Values were reported as means ± standard deviation (SD) unless otherwise indicated. Independent samples *t*-test and intraclass correlation coefficient (ICC) were used to test the feasibility of the global and 9 zonal vBMDs. Pearson's test was used to test the correlation between global vBMD, zonal vBMD, age, and BMI. One-way analysis of variance (ANOVA) was used to compare the difference of the global vBMD among the 3 age groups, and then the least significant difference (LSD) test was employed for post hoc multiple comparisons. The statistical methods used for comparison of age, BMI, and zonal vBMDs were the same as those employed for global vBMD. ANOVA was used to compare the difference of regional trabecular vBMD in the same age group, and then Dunnett's test was employed for post hoc multiple comparisons. Statistical significance was considered when $P<0.05$.

Results

Feasibility of global and 9 zonal vBMDs

There was no significantly difference of the global vBMD measured by the 2 analysts, and so as to the 9 zonal vBMDs measured by the 2 analysts ($P\geq0.638$), and the ICCs were all greater than or equal to 0.990 (*Table 1*).

Correlation between global vBMD, zonal vBMDs, age, and BMI

Age, BMI, global vBMD, and the zonal vBMDs were recorded and stratified into the 3 age groups (*Table 2*). There was no difference of BMI among the 3 age groups,

Table 1 Feasibility of global and nine zonal vBMD measured by 2 analysts

Global and zonal vBMDs	vBMD, mean ± SD (mg/cm^3)		*t*/*P**	ICC (95% CI)
	Analyst 1	Analyst 2		
Global vBMD	91.27±43.72	93.84±44.52	0.226/0.822	0.998 (0.997–0.999)
vBMD-ua	80.59±42.29	85.62±43.82	0.452/0.653	0.990 (0.979–0.995)
vBMD-um	86.23±43.02	90.60±45.44	0.383/0.703	0.996 (0.992–0.998)
vBMD-up	93.39±42.92	96.42±46.58	0.263/0.794	0.994 (0.987–0.997)
vBMD-ma	89.61±47.32	91.98±47.68	0.193/0.847	0.997 (0.993–0.998)
vBMD-mm	103.62±43.77	107.40±43.52	0.335/0.738	0.997 (0.994–0.999)
vBMD-mp	121.15±47.53	127.21±51.52	0.473/0.638	0.993 (0.986–0.997)
vBMD-la	79.40±45.46	82.60±47.69	0.266/0.791	0.992 (0.984–0.996)
vBMD-lm	85.65±46.45	91.22±49.01	0.452/0.653	0.995 (0.989–0.997)
vBMD-lp	109.90±43.10	113.38±48.20	0.295/0.769	0.990 (0.978–0.995)

*, independent samples *t*-test between 2 analysts. Global vBMD, global volumetric bone mineral density of the first lumbar vertebral body (L1); vBMD-ua, vBMD-um, vBMD-up, vBMD-ma, vBMD-mm, vBMD-mp, vBMD-la, vBMD-lm, and vBMD-lp are the abbreviations of vBMD for the upper and anterior, upper and middle, upper and posterior, middle and anterior, middle and middle, middle and posterior, lower and anterior, lower and middle and lower and posterior third of L1. vBMD, volumetric bone mineral density; ICC, intraclass correlation coefficient; CI, confidence interval.

whereas there was significant difference of global vBMD among the 3 age groups (P<0.001), and so as to the 9 zonal vBMDs among the 3 age groups (P<0.001).

Age was not correlated with BMI (r=0.055, P=0.190) and negatively correlated with global vBMD, vBMD-ua, vBMD-um, vBMD-up, vBMD-ma, vBMD-mm, vBMD-mp, vBMD-la, vBMD-lm, and vBMD-lp (r ranging from −0.400 to −0.610; all P<0.001). BMI was not correlated with the global vBMD and 9 zonal vBMDs (r ranging from −0.001 to −0.47, all P>0.05).

Comparison of regional vBMDs

There were significant differences among the vBMD-A, vBMD-M, and vBMD-P of each age group, and vBMD-A and vBMD-M were both lower than vBMD-P in each age group (*Table 3* and *Figure 3*). There were significant differences among vBMD-U, vBMD-M', and vBMD-L of each age group, and vBMD-U and vBMD-L were both lower than vBMD-M' in each age group (*Table 3* and *Figure 4*).

Discussion

QCT has been used to estimate vBMD for nearly 30 years (6), and estimated vBMDs using QCT for the cancellous regions are affected by acquisition protocols, such as X-ray tube peak voltage, table height, thickness, and reconstruction algorithm. In previous studies, variations of vBMDs in kilovoltage peak and table height were controlled for using a calibration phantom scanned at the same energy and height (7,8). In our study, we used the same CT scanning equipment, fixed voltage, table height, and reconstruction algorithm. QCT was calibrated with the European calibration phantom before the study to ensure the consistency and reliability of the trabecular vBMD data. First, we divided the L1 vertebral body into 9 zones according to the method of trisection of L1 at the maximum sagittal and axial plane. To minimize the influence of the vertebral vein on the zonal vBMDs, we segmented the vertebral body into 9 zones (that is 3 aliquots on axial plane, 3 aliquots on sagittal plane, similar to a three by three Rubik's cube). With the development of computer artificial intelligence (AI)-assisted technology, it may be possible to prepare more sections of the vertebrae to analyze the zonal vBMDs in the future, similar to finite element analysis, dividing the vertebrae into several grids, but the required computer AI-assisted technology remains to be developed. There were no significant differences in the 9 zonal vBMDs measured by the 2 analysts, and ICC were all ≥0.990. Thus, the results of our study demonstrated that the 9 zonal

Table 2 Age, body mass index, global vBMD and zonal vBMDs distribution of the three age groups

Clinical parameters and vBMD	50–59 years	60–69 years	70–80 years	*F*/*P**
n	196	214	168	–
Age (years)	54.63±3.07$^{\&\eta}$	64.13±2.83$^{\#}$	74.67±3.02	2,059.816/<0.001
BMI (kg/m^2)	24.60±3.83	25.05±3.54	24.55±3.44	1.158/0.315
Global vBMD (mg/cm^3)	120.72±39.86$^{\&\eta}$	88.82±30.85$^{\#}$	69.25±27.02	112.618/<0.001
vBMD-ua (mg/cm^3)	104.39±34.63$^{\&\eta}$	75.59±26.23$^{\#}$	55.87±24.39	130.959/<0.001
vBMD-um (mg/cm^3)	115.37±39.14$^{\&\eta}$	85.10±30.82$^{\#}$	64.44±24.51	115.095/<0.001
vBMD-up (mg/cm^3)	124.12±42.55$^{\&\eta}$	93.21±33.08$^{\#}$	73.63±28.12	95.468/<0.001
vBMD-ma (mg/cm^3)	119.83±39.38$^{\&\eta}$	87.44±32.54$^{\#}$	65.16±27.69	121.515/<0.001
vBMD-mm (mg/cm^3)	133.90±42.73$^{\&\eta}$	102.12±34.08$^{\#}$	82.62±32.66	90.775/<0.001
vBMD-mp (mg/cm^3)	152.75±49.77$^{\&\eta}$	120.45±41.66$^{\#}$	104.62±44.51	54.234/<0.001
vBMD-la (mg/cm^3)	106.83±38.51$^{\&\eta}$	74.52±27.30$^{\#}$	53.13±21.08	147.837/<0.001
vBMD-lm (mg/cm^3)	117.81±42.58$^{\&\eta}$	84.70±30.52$^{\#}$	62.93±23.23	125.658/<0.001
vBMD-lp (mg/cm^3)	145.17±48.92$^{\&\eta}$	110.35±35.21$^{\#}$	89.08±30.51	95.859/<0.001

Values are presented as mean ± standard deviation. vBMD-ua, vBMD-um, vBMD-up, vBMD-ma, vBMD-mm, vBMD-mp, vBMD-la, vBMD-lm, and vBMD-lp are the abbreviations of vBMD for the upper and anterior, upper and middle, upper and posterior, middle and anterior, middle and middle, middle and posterior, lower and anterior, lower and middle, and lower and posterior third of L1. *: ANOVA was used to compare the differences among the three age groups. $^{\&}$, $^{\#}$ and $^{\eta}$: least significant difference test for post hoc multiple comparisons and there was difference. $^{\&}$ and $^{\#}$: compared with 70–80 years, $^{\eta}$: compared with 60–69 years. BMI, body mass index; vBMD, volumetric bone mineral density; ANOVA, one-way analysis of variance.

Table 3 Distribution and comparison of six regional volumetric bone mineral density of three age groups

Regional vBMD	50–59 years	60–69 years	70–80 years
vBMD-A (mg/cm^3)	110.35±36.29*	79.18±27.27*	58.05±22.96*
vBMD-M (mg/cm^3)	122.36±40.38*	90.64±30.50*	70.00±25.09*
vBMD-P (mg/cm^3)	140.68±45.69	108.00±34.85	89.11±32.08
F/P$^{\$1}$	27.250/<0.001	46.793/<0.001	56.595/<0.001
vBMD-U (mg/cm^3)	114.63±37.90$^{\&}$	84.63±28.93$^{\&}$	64.64±24.24$^{\&}$
vBMD-M' (mg/cm^3)	135.49±42.58	103.34±34.39	84.13±33.42
vBMD-L (mg/cm^3)	123.27±42.31$^{\&}$	89.86±29.68$^{\&}$	68.38±23.31$^{\&}$
F/P$^{\$2}$	12.824/<0.001	20.619/<0.001	23.991/<0.001

Values are presented as mean ± standard deviation. vBMD-A, vBMD-M, and vBMD-P were defined as vBMD of the anterior, middle, and posterior third of the first lumbar vertebral body (L1). vBMD-U, vBMD-M', and vBMD-L were defined as vBMD of the upper, middle, and lower third of L1. $^{\$1}$: ANOVA was used to compare the difference of vBMD-A, vBMD-M, and vBMD-P, and then the Dunnett test (compared with vBMD-P) for post hoc multiple comparisons. $^{\$2}$: ANOVA was used to compare the differences between vBMD-U, vBMD-M', and vBMD-L, and then Dunnett's test (compared with vBMD-M') for post hoc multiple comparisons. *: there was a difference compared with the vBMD-P. $^{\&}$: there was a difference compared with the vBMD-M'. vBMD, volumetric bone mineral density; ANOVA, one-way analysis of variance.

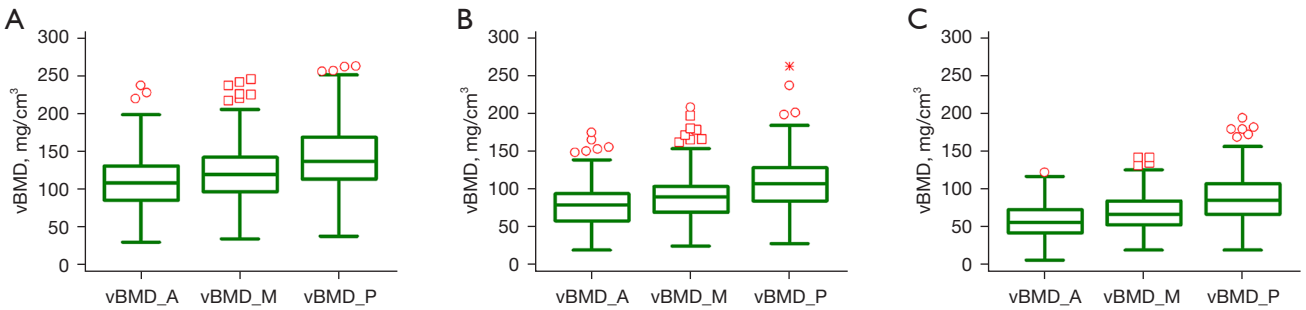

Figure 3 Boxplot showing the comparison among vBMD-A, vBMD-M, and vBMD-P of each age group. ANOVA was used to compare the difference among vBMD-A, vBMD-M, and vBMD-P of each age group, and then Dunnett's test for post hoc multiple comparisons, whereby vBMD-A and vBMD-M were both compared with vBMD-P. (A) 50–59 years; (B) 60–69 years; (C) 70–80 years. P: Dunnett's test. *: outlier of vBMD-P, which was equal to 263.45 mg/cm^3. vBMD-A, vBMD-M, and vBMD-P were defined as vBMD for the anterior, middle, and posterior third of L1 from the ventral to the dorsal side of L1 vertebral body. vBMD, volumetric bone mineral density; ANOVA, one-way analysis of variance.

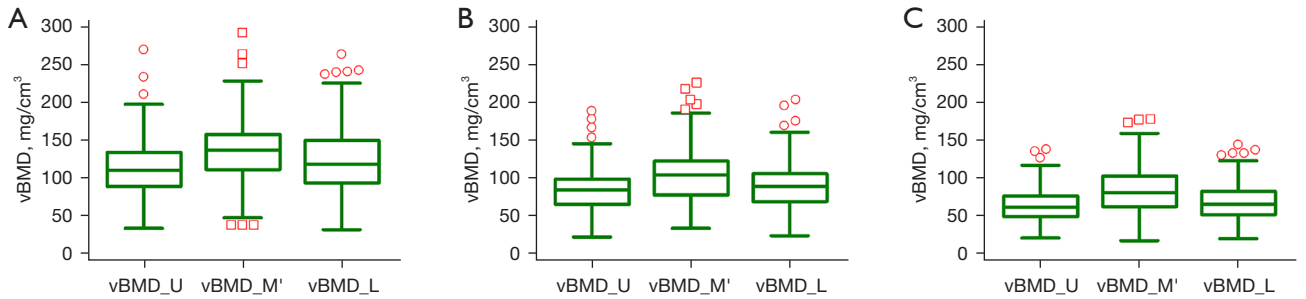

Figure 4 Boxplot showing the comparison among vBMD-U, vBMD-M', and vBMD-L of each age group. ANOVA was used to compare the difference among vBMD-U, vBMD-M', and vBMD-L of each age group, and then Dunnett's test for post hoc multiple comparisons, whereby vBMD-U and vBMD-L were both compared with vBMD-M'. (A) 50–59 years; (B) 60–69 years; (C) 70–80 years. P: Dunnett's test. vBMD-U, vBMD-M', and vBMD-L were defined as vBMD for the upper, middle, and lower third of L1 from the head to the foot of the L1 vertebral body. vBMD, volumetric bone mineral density; ANOVA, one-way analysis of variance.

trabecular vBMD method was feasible and available.

Previous studies have shown that BMD decreases with age (9-11). Consistent with the above results, the present study showed that the global vBMD was negatively correlated with age. The loss of BMD in women consists of 2 stages, which begin after menopause, as a quick estrogen-dependent process with a rapid decrease in bone mass lasting about 5–10 years during which about 50% of the total BMD of the spine is lost, and after this period, a slow, constant, age-related loss follows. Hormonal imbalance, aging, environmental factors, lifestyle, and genetic predisposition are responsible for about 50–80% of BMD loss. The annual bone mass loss amounts to about 0.5% in premenopausal women, 2–2.5% in women going through menopause, and about 1.5% in postmenopausal women (12). Research results indicate a significant role of BMI in maintaining BMD appropriate for a given age (13,14). There is no significant correlation between global vBMD and BMI. A previous study showed that adipose tissue might influence vBMD through the production of hormones and adipokines by adipocytes or through an effect on the secretion of bone-active hormones from the pancreas (15). Nevertheless, adipose tissue is metabolically heterogeneous, with differences between subcutaneous adipose and visceral adipose tissue, whereas BMI cannot adequately distinguish between the 2 tissue types (16).

The vBMD derived from QCT can be used for diagnosis of osteopenia, which is defined as vBMD from 80 to 120 mg/cm^3, or osteoporosis, which is defined as vBMD less than 80 mg/cm^3, respectively (17). Osteopenia and

osteoporosis are the major risk factors for osteoporotic vertebral deformity (OVD) (18). OVD usually includes 3 types: crush, wedge, and biconcave deformities (19,20). In the present study, vBMD-A and vBMD-M of L1 were both lower than vBMD-P in each age group, which may quantitatively explain the vertebral wedge deformity from the perspective of BMD. Both vBMD-U and vBMD-L were lower than vBMD-M' in each age group, which may quantitatively explain the vertebral biconcave deformity from the perspective of BMD. At present, vBMD measured using QCT software is the central region of the vertebral cancellous bone, as shown in *Figure 2A*. The vBMD of the vertebral central area cannot represent the edge of the vertebral body. Some patients with normal vertebral central vBMD have chest and back pain or severe deformation in the absence of trauma, surgery, or spine arthritis; our study also showed that the vBMD of the vertebral central area was the highest, and that vBMD measured using QCT software may overlook early osteopenia and osteoporosis. Our study relied on QCT software to segment vertebral bodies into 9 zones and then calculated the mean vBMD of different regions, which may explain the common wedge and biconcave deformity of the vertebral body from the perspective of cancellous vBMD. However, the ability of bone to resist deformity and/or fracture is known as bone strength and depends not just on BMD but also on bone quality, which relates to such factors as bone architecture, turnover, mineralization, and cellularity (21). Structures (such as muscles, ligaments, and adnexal bones of the spinal posterior column) designed to resist OVD were also not considered. Only the vBMD was researched to elucidate the mechanism of vertebral wedge and biconcave deformity, and further studies are needed.

Limitations

Our study has several limitations. First, this was a retrospective study, and additional prospective and multicenter studies are required to independently validate these results. Second, we only analyzed global vBMD and regional vBMDs of L1, whereas previous studies have generally selected the average vBMD of 2 or 3 lumbar vertebral bodies. Third, we only studied the vBMD for OVD, and other factors (like bone architecture, cortical, bone strength, and bone transformation) have not been taken into consideration. Finally, most of our patients did not undergo DXA, and zonal vBMDs could not be compared with the results of DXA to assess the value of zonal vBMDs in diagnosing osteopenia or osteoporosis. Moreover, the data on time used for analyzing 1 patient was not collected, and we will record the time taken to measure the zonal vBMDs for each patient in future work.

Conclusions

We demonstrated the feasibility of the 9 zonal trabecular vBMD method in L1. The 9 zonal trabecular vBMD method may quantitatively explain osteoporotic vertebral deformity from the perspective of vBMD in middle-aged and elderly women.

Acknowledgments

Funding: This study was supported by the Natural Science Foundation of Hebei Province (No. H2018206273).

Footnote

Conflicts of Intertest: All authors have completed the ICMJE uniform disclosure form (available at https://qims.amegroups.com/article/view/10.21037/qims-22-575/coif). The authors have no conflicts of interest to declare.

Ethical Statement: The authors are accountable for all aspects of the work in ensuring that questions related to the accuracy or integrity of any part of the work are appropriately investigated and resolved. The study was conducted in accordance with the Declaration of Helsinki (as revised in 2013). The study was approved by the ethics committee of the Third Hospital of Hebei Medical University (No. ke2018-036-1). Informed consent was provided by all patients for this study.

References

1. Wáng YXJ, Xiao BH. Estimations of bone mineral density

defined osteoporosis prevalence and cutpoint T-score for defining osteoporosis among older Chinese population: a framework based on relative fragility fracture risks. Quant Imaging Med Surg 2022;12:4346-60.
2. Yuan HA, Brown CW, Phillips FM. Osteoporotic spinal deformity: a biomechanical rationale for the clinical consequences and treatment of vertebral body compression fractures. J Spinal Disord Tech 2004;17:236-42.
3. Genant HK, Wu CY, van Kuijk C, Nevitt MC. Vertebral fracture assessment using a semiquantitative technique. J Bone Miner Res 1993;8:1137-48.
4. Woisetschläger M, Hägg M, Spångeus A. Computed tomography-based opportunistic osteoporosis assessment: a comparison of two software applications for lumbar vertebral volumetric bone mineral density measurements. Quant Imaging Med Surg 2021;11:1333-42.
5. Abdalbary M, Sobh M, Elnagar S, Elhadedy MA, Elshabrawy N, Abdelsalam M, Asadipooya K, Sabry A, Halawa A, El-Husseini A. Management of osteoporosis in patients with chronic kidney disease. Osteoporos Int 2022;33:2259-74.
6. Sandor T, Felsenberg D, Kalender WA, Clain A, Brown E. Compact and trabecular components of the spine using quantitative computed tomography. Calcif Tissue Int 1992;50:502-6.
7. Giambini H, Dragomir-Daescu D, Huddleston PM, Camp JJ, An KN, Nassr A. The Effect of Quantitative Computed Tomography Acquisition Protocols on Bone Mineral Density Estimation. J Biomech Eng 2015;137:114502.
8. Smith KE, Whiting BR, Reiker GG, Commean PK, Sinacore DR, Prior FW. Assessment of technical and biological parameters of volumetric quantitative computed tomography of the foot: a phantom study. Osteoporos Int 2012;23:1977-85.
9. Torgutalp ŞŞ, Babayeva N, Kara ÖS, Özkan Ö, Dönmez G, Korkusuz F. Trabecular bone score of postmenopausal women is positively correlated with bone mineral density and negatively correlated with age and body mass index. Menopause 2019;26:1166-70.
10. Gao L, Zhang P, Wang Y, Zhang W, Zhao J, Liu Y, Liu J, He S. Relationship between body composition and bone mineral density in postmenopausal women with type 2 diabetes mellitus. BMC Musculoskelet Disord 2022;23:893.
11. Tang H, Di W, Qi H, Liu J, Yu J, Cai J, Lai B, Ding G, Cheng P. Age-Related Changes in Trabecular Bone Score and Bone Mineral Density in Chinese Men: A Cross-Sectional and Longitudinal Study. Clin Interv Aging 2022;17:429-37.
12. Syed FA, Ng AC. The pathophysiology of the aging skeleton. Curr Osteoporos Rep 2010;8:235-40.
13. Skrzek A, Kozieł S, Ignasiak Z. The optimal value of BMI for the lowest risk of osteoporosis in postmenopausal women aged 40-88 years. Homo 2014;65:232-9.
14. De Laet C, Kanis JA, Odén A, Johanson H, Johnell O, Delmas P, Eisman JA, Kroger H, Fujiwara S, Garnero P, McCloskey EV, Mellstrom D, Melton LJ 3rd, Meunier PJ, Pols HA, Reeve J, Silman A, Tenenhouse A. Body mass index as a predictor of fracture risk: a meta-analysis. Osteoporos Int 2005;16:1330-8.
15. Reid IR. Relationships between fat and bone. Osteoporos Int 2008;19:595-606.
16. Singhal V, Bose A, Liang Y, Srivastava G, Goode S, Stanford FC, Misra M, Bredella MA. Marrow adipose tissue in adolescent girls with obesity. Bone 2019;129:115103.
17. Cheng X, Zhao K, Zha X, Du X, Li Y, Chen S, et al. Opportunistic Screening Using Low-Dose CT and the Prevalence of Osteoporosis in China: A Nationwide, Multicenter Study. J Bone Miner Res 2021;36:427-35.
18. Morosano ME, Menoyo I, Caferra DA, Sánchez A, Tomat MF, Bocanera R, Pezzotto SM, Masoni AM. Vulnerability of healthy vertebrae in patients with and without previous vertebral fracture. Bone 2011;48:820-7.
19. Ismail AA, Cooper C, Felsenberg D, Varlow J, Kanis JA, Silman AJ, O'Neill TW. Number and type of vertebral deformities: epidemiological characteristics and relation to back pain and height loss. European Vertebral Osteoporosis Study Group. Osteoporos Int 1999;9:206-13.
20. Xia W, Liu Q, Lv J, Zhang Z, Wu W, Xie Z, Chen J, He L, Dong J, Hu Z, Lin Q, Yu W, Wei F, Wang J. Prevalent vertebral fractures among urban-dwelling Chinese postmenopausal women: a population-based, randomized-sampling, cross-sectional study. Arch Osteoporos 2022;17:120.
21. Kristensen SV, Outzen C, Grau LM, Larsen TR, Bidstrup M, Egeskjold MV, Knude JA, Juhl D, Precht H. Can advanced edge enhancement software improve image quality to visualise tubes, catheters and wires in digital chest radiographs? Radiography (Lond) 2023;29:165-70.

Cite this article as: Yang X, Liu Y, Liu J, Gao L, Zhang P, Wang Y, Zhang W. Quantitative assessment of zonal trabecular volumetric bone mineral density in middle-aged and elderly women using quantitative computed tomography. Quant Imaging Med Surg 2023;13(4):2278-2286. doi: 10.21037/qims-22-575

